PHYSICAL REVIEW B VOLUME 15, NUMBER 4 15 FEBRUARY 1977

Self-consistent pseudopotential calculation of the electronic structure of Nb[†]

K. M. Ho, Steven G. Louie,[*] James R. Chelikowsky,[‡] and Marvin L. Cohen

Department of Physics, University of California and Materials and Molecular Research Division,
Lawrence Berkeley Laboratory, Berkeley, California 94720

(Received 12 October 1976)

The electronic structure of Nb is calculated using a self-consistent pseudopotential method. The calculated band structure and density of states are in good agreement with augmented-plane-wave calculations and with photoemission measurements. The total electronic charge density and partial charge densities for specific energy regions are presented and discussed.

INTRODUCTION

We present a self-consistent calculation of the electronic structure of bulk Nb using the pseudopotential method. Non-self-consistent band-structure calculations have been done for Nb using the modified orthogonalized-plane-wave method,[1] the augmented-plane-wave method (APW),[2] the empirical-pseudopotential method (EPM)[3] and the plane-wave-Gaussian method.[4] All these calculations are generally in good agreement with each other and with Fermi-surface experiments.[5] Using a Slater-Koster parametrization of the APW band structure, Pickett and Allen[6] have recently calculated a joint density of states for Nb which agrees reasonably well with the imaginary part of of the dielectric function $\epsilon_2(\omega)$ obtained from experimental reflectivity data.[7] A self-consistent APW calculation by Anderson *et al.*[8] gives results differing significantly from other calculations particularly at the H point in the Brillouin zone.

A similar approach to the self-consistent method used here has been applied to localized configurations.[9] In particular, this method has recently been applied to calculations of surface and interface properties of semiconductors and simple metals,[10] where self-consistency is important. Self-consistency is also very important for transition-metal surfaces as has been shown in previous calculations.[11]

In the following, we will first give an outline of our method of calculation and then present results for the Nb band structure and density of states. We obtained results consistent with experimental measurements[5,12] and previous non-self-consistent calculations.[1-4] We will also present charge distributions for the total valence electrons and also for states in particular energy ranges.

METHOD OF CALCULATION

The electronic band structure of Nb was calculated from a pseudopotential Hamiltonian

$$H = p^2/2m + V_{\text{ps}} + V_H + V_x \quad , \tag{1}$$

where V_{ps} is a weak pseudopotential taken to be a superposition of Nb^{+5} ionic pseudopotentials

$$V_{\text{ps}}(\vec{r}) = \sum_{\vec{R}_n} V_{\text{ps}}^{\text{ion}}(\vec{r} - \vec{R}_n) \tag{2}$$

and

$$V_{\text{ps}}^{\text{ion}} = \sum_{l=0}^{2} V_l P_l \quad , \tag{3}$$

where P_l is the projection operator acting on the lth angular momentum component of the wave function. The nonlocal Nb^{+5} pseudopotential takes into account the differences in the repulsive potentials that each angular momentum component sees as a result of core orthogonalization.

V_s, V_p, V_d are chosen to reproduce both the experimental *ionic* levels (obtained from the spectra of Nb^{+4},[13] i.e., the Nb^{+5} core plus one electron system) and the positions of the peaks of the $4d$ and $5s$ *atomic* wave functions (compared to Herman-Skillman values[14]). A comparison of our results with those from experiment and Herman and Skillman is given in Table I. Figure 1 is a plot of our V_s, V_p, and V_d ionic pseudopotentials. It can be seen that the d electrons feel a much weaker core orthogonalization repulsion than the s and p electrons.

The ionic pseudopotential is screened by adding a Hartree potential V_H and a local exchange potential V_x obtained from the charge density ρ by

$$\nabla^2 V_H(\vec{r}) = -4\pi e^2 \rho(\vec{r}) \quad , \tag{4}$$

and

$$V_x = -3e^2(3/8\pi)^{1/3} \alpha \rho(\vec{r})^{1/3} \quad . \tag{5}$$

In the present calculation, the value of the exchange parameter α was chosen to be 0.8, however the results are not very sensitive to this value. Shifts of d states of ~0.1 eV occur for a change of 0.1 in α.

The iteration procedure is started by approxi-

TABLE I. (a) Comparison of the calculated ionic energy levels with experimental data (Ref. 13). (b) Self-consistent Nb atom: energy levels and peaks of atomic wave functions. A comparison of our results with those of Herman and Skillman.

Level	Nb^{+4} Calculated energy (Ry)	Expt. energy (Ry)
4*d*	−3.657	−3.63
5*s*	−2.953	−2.95
5*p*	−2.448	−2.45
5*d*	−1.725	−1.71
6*s*	−1.635	−1.56

Self-consistent Nb atom energies (Ry)

	Present calculation	Herman and Skillman
4*d*	0.354	0.45
5*s*	0.340	0.40

Positions of maximum of $rR(r)$ (a.u.)

	Present calculation	Herman and Skillman
4*d*	1.48± 0.02	1.41
5*s*	3.00 ± 0.05	3.12

mating the $V_{ps}+V_H+V_x$ term in the Hamiltonian by a pseudopotential constructed from a superposition of atomic pseudopotentials. With this Hamiltonian, the valence charge distribution is calculated and from it the screening potentials V_H and V_x are obtained. V_H and V_x are then put back into the Hamiltonian. The procedure is repeated until self-consistency is reached, i.e., until the input and output screening potentials V_H+V_x agree with each other.

The wave function was expanded in a basis set of ~80 plane waves (corresponding to a maximum energy of 10.2 Ry), a further 80 waves were included by second-order perturbation up to an energy of 16.0 Ry. Convergence tests showed that *s* and *p* levels and separations between *d* levels converged to <0.01 eV while *d* levels may shift relative to *s* and *p* levels by as much as 0.2 eV with the inclusion of more plane waves in the basis set.

In the iteration towards self-consistency, energy eigenvalues were calculated for a grid of eight special points[15] in the irreducible bcc Brillouin zone. The Fermi level E_F is then determined by

$$2\sum_{\vec{k}_i}\sum_{n} W_{\vec{k}_i}\Theta(E_F - E_n(\vec{k}_i)) = z \ , \qquad (6)$$

where z is the number of electrons per primitive cell (five in the case of bulk Nb). $W_{\vec{k}_i}$ is the weight for each special point k_i,[15] and Θ is the Heaviside step function.

The valence charge density is calculated from

$$\rho(\mathbf{r}) = 2\sum_{\vec{k}\in \mathrm{BZ}}\ \sum_{\substack{n \\ E_n(\vec{k})\le E_F}} \psi^*_{n,\vec{k}}(\vec{r})\psi_{n,\vec{k}}(\vec{r}) \ . \qquad (7)$$

A total of 370 plane waves were used in expanding the charge density corresponding to a cutoff energy of 30.0 Ry.

With the self-consistent potential, the energy eigenvalues were calculated at 285 $\vec{k}$ points in the irreducible Brillouin zone. For bulk Nb, this gives the band structure, the density of states, the valence charge distribution, and the charge distributions for states under the various peaks in the density of states.

RESULTS

The band structure $E_n(\vec{k})$ is plotted along symmetry directions of the bcc Brillouin zone in Fig.

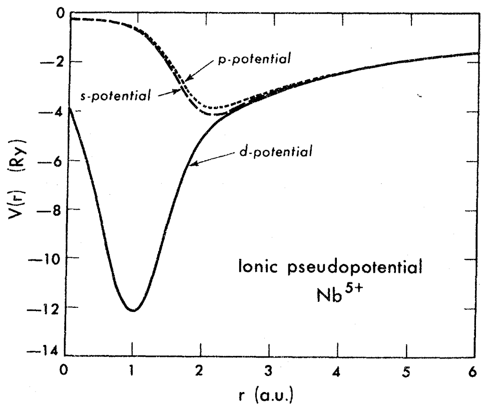

FIG. 1. Nb^{+5} ionic pseudopotentials V_s, V_p, and V_d plotted as a function of r.

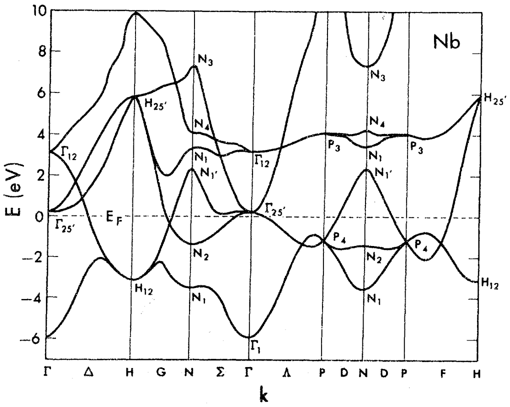

FIG. 2. Electronic band structure of niobium. The zero of energy is at the Fermi energy E_F.

TABLE II. Comparison of important energy levels for Nb between the present results and previous calculations (in eV, $E_F = 0$).

	Γ_1	$\Gamma_{25'}$	Γ_{12}	H_{12}	$H_{25'}$	$N_{1'}$
Predominant character	*s*	*d*	*d*	*d*	*d*	*p*
Present calc.	−6.06	0.15	3.07	−3.22	5.83	2.32
APW (Ref. 2)	−5.30	0.41	2.80	−3.81	5.17	2.33
EPM (Ref. 3)	−5.20	0.51	2.59	−3.70	5.68	2.18
Self-consistent (Ref. 8) APW	−5.24	0.55	3.25	−4.24	5.97	2.25

2. This result is in good agreement with the results of previous band calculations.[1−4,8] Table II compares the principal energy levels of the present band structure with those of previous calculations. The main differences are the lowest Γ_1 level for the present calculation is ~0.8 eV lower than previous results and the $\Gamma_{12} - \Gamma_{25'}$ gap is ~0.8 eV larger.

The histogram density of states for the present calculation is shown in Fig. 3(a). It is in good agreement with Mattheiss's APW calculation[2] [Fig. 3(b)] and the photoemission data of Eastman.[12]

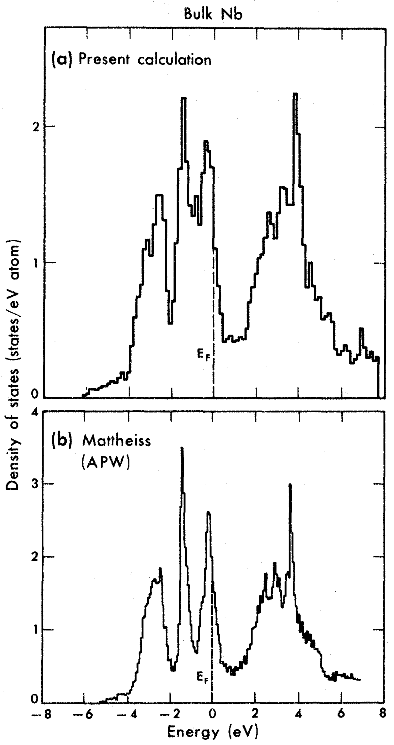

FIG. 3. Density of states of (a) present calculation (b) APW calculation by Mattheiss (Ref. 2).

Table III gives the positions of the peaks in the density of states of the present calculation and comparison with previous results and experiment. The value of $N(E_F)$ obtained in the present calculation is 1.1 states/(eV atom) as compared with the empirical value 0.91 states/(eV atom) obtained by McMillan.[16]

The distribution of the valence electrons in the (110) and (100) planes are shown in Fig. 4. The positions of the Nb atoms are indicated by black dots. The charge density is zero at the atom because of the highly repulsive core. It then rises up sharply to form lobes around the atoms showing distinct *d*-like character. The position of the peaks in the *d*-electron charge density is approximately the same as the position of the peak of the *d*-electrons in the isolated Nb atom. In addition to the lobes, there is a uniform charge background in the space between the atoms.

Plotting the charge distributions for states under the various peaks in the density of states reveal that they have different characteristics. The total charge distribution for states under the lowest peak *A* with energies from −6.0 to −2.0 eV is shown in Fig. 5(a). The charge distribution is mainly *s*-like with a bit of $d_{3z^2-r^2}$ character. The

TABLE III. Energy values for principal peak positions in the density of states are compared with peaks in photoemission data (Ref. 12) and APW (Ref. 2) and EPM (Ref. 3) results (in electron volts).

Experiment (Photoemission) (Ref. 12)	Theory APW (Ref. 2)	EPM (Ref. 3)	Present calculation
−2.3	−2.4	−2.6	−2.5
−1.1	−1.4	−1.4	−1.4
−0.4	−0.2	−0.4	−0.4
⋯	2.5	⋯	2.6
⋯	3.0	⋯	3.2
⋯	3.7	2.6	3.8

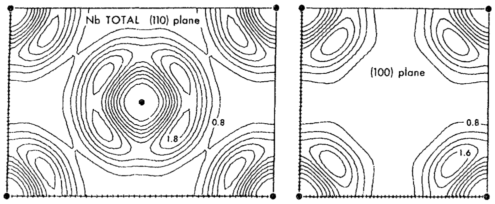

FIG. 4. Contour plots of total valence charge distribution of Nb in the (110) and (100) planes. The charge is normalized to one electron per unit cell.

charge distributions for peak B (−2.0 to −0.75 eV) and peak C (−0.75 to 0.60 eV), shown in Figs. 5(b) and 5(c), look alike with the charge concentrated mainly in bonding d-like lobes along the line joining two neighboring atoms. The charge for the highest and unoccupied peak D (0.60 to 5.85 eV) has distinct $d_{3z^2-r^2}$ and $d_{x^2-y^2}$ character around each atomic site.

In our calculation, we have not adjusted our Fermi surface to fit experiments. The calculated Fermi surface is in satisfactory agreement with previous calculations[2,3,5,8] with one exception. In contrast to APW calculations[2] and de Haas–van Alphen experiments,[5] the Fermi surface in the present calculation does not cut across the Σ symmetry line ($\Gamma - N$). This can be seen from the band structure in Fig. 2; the third band along the Σ direction, just misses cutting the Fermi by ~0.1 eV. We did not make this minor adjustment in the present calculation, but it should be considered if calculations of Fermi surface structure are done.

CONCLUSION

In summary we have presented a calculation of the band structure of Nb using the self-consistent pseudopotential method and obtained results consistent with Mattheiss's APW calculation[2] and experiments.[5,12] This demonstrates the applicability of the present pseudopotential method which can be used as a base for calculating the surface properties of Nb and other applications like band-structure calculations of compounds with Nb as a constituent atom.

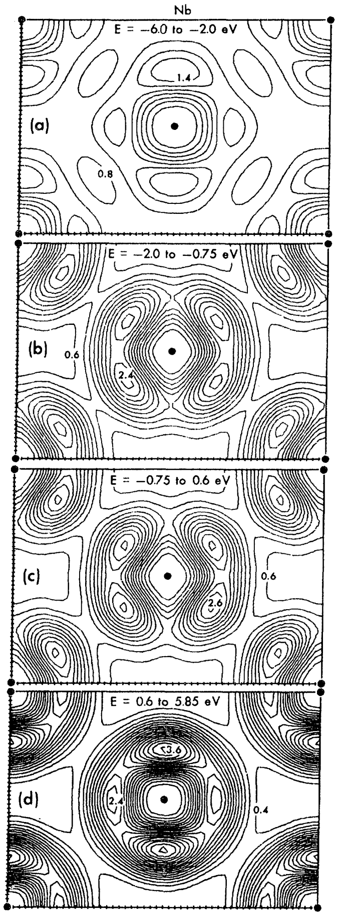

FIG. 5. Partial charge densities for states in the energy ranges (a) −6.0 to −2.0 eV, (b) −2.0 to −0.75 eV, (c) −0.75 to 0.60 eV, and (d) 0.60 to 5.85 eV. The charges are normalized to one electron per unit cell.

ACKNOWLEDGMENT

Part of this work was done under the auspices of the United States Energy Research and Development Administration.

---

*Supported in part by the NSF.

†Supported in part by the NSF Grant No. DMR72-03206-A02.

‡Present address: Bell Telephone Laboratories, Murray Hill, N. J. 07974.

[1] R. A. Deegan and W. D. Twose, Phys. Rev. 164, 993 (1967).

[2] L. F. Mattheiss, Phys. Rev. B 1, 373 (1970).

[3] C. Y. Fong and M. L. Cohen, Phys. Lett. A 44, 375 (1973).

[4] R. N. Euwema, Phys. Rev. B 4, 4332 (1971).

[5] M. H. Halloran, J. H. Condon, J. E. Graebner, J. E. Kunzler, and F. S. L. Hsu, Phys. Rev. B 1, 366 (1970).

[6] W. E. Pickett and P. B. Allen, Phys. Rev. B 11, 3599 (1975).

[7] J. H. Weaver, D. W. Lynch, and C. G. Olson, Phys. Rev. B 7, 4311 (1973).

[8] J. R. Anderson, D. A. Papaconstantopoulos, J. W. McCaffrey, and J. E. Schirber, Phys. Rev. B 7, 5115 (1973).

[9] M. L. Cohen, M. Schlüter, J. R. Chelikowsky, and S. G. Louie, Phys. Rev. B 12, 5575 (1975). Self-consistent bulk calculations are done first and the results are then used for application to localized configurations.

[10] M. Schlüter, J. R. Chelikowsky, S. G. Louie, and M. L. Cohen, Phys. Rev. B 12, 4200 (1975); J. R. Chelikowsky, M. Schlüter, S. G. Louie, and M. L. Cohen, Solid State Commun. 17, 1103 (1975); S. G. Louie and M. L. Cohen, Phys. Rev. B 13, 2461 (1976).

[11] E. Caruthers and L. Kleinman, Phys. Rev. Lett. 35, 738 (1975).

[12] D. E. Eastman, Solid State Commun. 7, 1697 (1969).

[13] C. E. Moore, Circ. U. S. Natl. Bur. Stand. 2, 467 (1952).

[14] F. Herman and S. Skillman, *Atomic Structure Calculations* (Prentice-Hall, Englewood Cliffs, N. J., 1963).

[15] D. J. Chadi and M. L. Cohen, Phys. Rev. B 8, 5747 (1973).

[16] W. L. McMillan, Phys. Rev. 167, 331 (1968).